Evaluating Stage Motion for Automated Electron Microscopy

Kevin R Fiedler, Matthew J Olszta, Kayla H Yano, Christina Doty, Derek Hopkins, Sarah Akers, Steven R Spurgeon

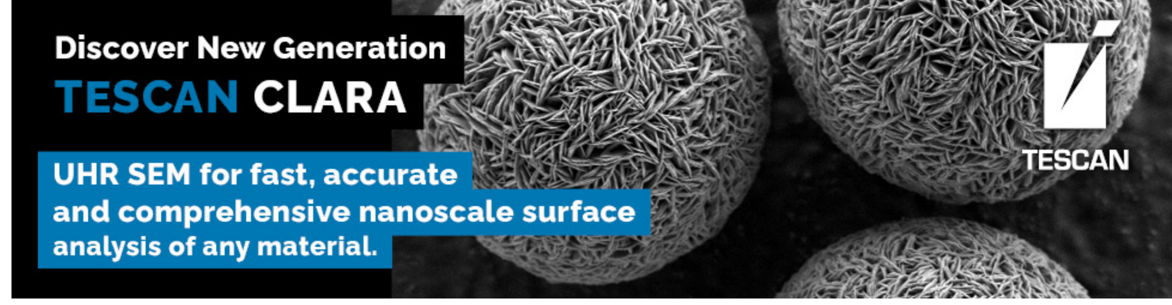

Downloaded from https://academic.oup.com/mam/advance-article/doi/10.1093/micmic/ozad108/7313517 by guest on 13 October 2023

Microscopy and Microanalysis, 2023, **00**, 1–9
https://doi.org/10.1093/micmic/ozad108

Microscopy AND Microanalysis

Original Article

Evaluating Stage Motion for Automated Electron Microscopy

Kevin R. Fiedler[1,2], Matthew J. Olszta[2], Kayla H. Yano[2], Christina Doty[3], Derek Hopkins[4], Sarah Akers[3], and Steven R. Spurgeon[2,5,*]

[1]*College of Arts and Sciences, Washington State University—Tri-Cities, Richland, WA 99354, USA*
[2]*Energy and Environment Directorate, Pacific Northwest National Laboratory, Richland, WA 99352, USA*
[3]*National Security Directorate, Pacific Northwest National Laboratory, Richland, WA 99352, USA*
[4]*Environmental Molecular Sciences Laboratory, Pacific Northwest National Laboratory, Richland, WA 99352, USA*
[5]*Department of Physics, University of Washington, Seattle, WA 98195, USA*

***Corresponding author:** Steven R. Spurgeon, E-mail: steven.spurgeon@pnnl.gov

Downloaded from https://academic.oup.com/mam/advance-article/doi/10.1093/micmic/ozad108/7313517 by guest on 13 October 2023

Abstract

Precise control is an essential and elusive quality of emerging self-driving transmission electron microscopes (TEMs). It is widely understood these instruments must be capable of performing rapid, high-volume, and arbitrary movements for practical self-driving operation. However, stage movements are difficult to automate at scale, owing to mechanical instability, hysteresis, and thermal drift. Such difficulties pose major barriers to artificial intelligence-directed microscope designs that require repeatable, precise movements. To guide design of emerging instruments, it is necessary to understand the behavior of existing mechanisms to identify rate limiting steps for full autonomy. Here, we describe a general framework to evaluate stage motion in any TEM. We define metrics to evaluate stage degrees of freedom, propose solutions to improve performance, and comment on fundamental limits to automated experimentation using present hardware.

Key words: automation, control system, electron microscopy, precision, stage motion

Introduction

Artificial intelligence (AI), encompassing disciplines such as robotics, machine learning (ML), and computer vision, has begun to transform the study of materials, chemical, and biological systems (Lalmuanawma et al., 2020; Sha et al., 2020; Batra et al., 2021). AI allows us to richly analyze more data and discover latent, multidimensional patterns that inform physical mechanisms, such as those underpinning quantum computing, energy storage, and designer medicine (Butler et al., 2018; Schmidt et al., 2019; Vasudevan et al., 2019; Battineni et al., 2020). Electron microscopy (EM), a pillar of characterization at high spatial and chemical resolution, stands to benefit greatly from these approaches (Ede, 2021; Kalinin et al., 2022; Treder et al., 2022). At present, most EM data collection and analysis is still conducted by hand, with limited subsets of data collected from large or rapidly changing samples. With the emergence of customized ML techniques and inexpensive edge computing hardware, it is now possible to analyze data in greater volume and depth. ML methods have shown success on a range of EM-related tasks, including segmentation (Akers et al., 2021; Groschner et al., 2021; Xu et al., 2021; Stuckner et al., 2022), automated instrument tuning (Xu et al., 2022), determination of microstructural descriptors (Laanait et al., 2016; Ziatdinov et al., 2017; Dan et al., 2022; Ziatdinov et al., 2022a), and in situ forecasting (Lewis et al., 2022). These methods are now beginning to grapple with the large volumes of data produced by modern detectors, yielding richer statistical insights into important chemical and materials systems (Spurgeon et al., 2021).

While new approaches for EM data analysis have been developed, their on-the-fly implementation on microscope hardware has been far slower. This situation is starting to be improved with the release of interactive programming modules (e.g., Python), which will eventually lead to findable, accessible, interoperable, and reusable (FAIR) microscopy (Wilkinson et al., 2016; Schorb et al., 2019; Kalinin et al., 2021). In the past, users were limited by the constraints of commercial software and analytical routines provided by each microscope or detector. Recently, there have been some notable successes in the development of more open microscope platforms and controllers, including systems driven by Gaussian process optimization (Liu et al., 2022; Ziatdinov et al., 2022b) and our own modular platform based on sparse data analytics (Olszta et al., 2022). In all cases, numerous decisions must be made regarding imaging conditions, sample movement/orientation, and detector configuration dictated by analytic requirements. In the most basic "open-loop" experiment, these decisions are hard-coded a priori and then executed without further adaptive feedback. While there are some scenarios in which an "open-loop" approach can be successful —such as large area, low magnification imaging of static samples—the approach is insufficient for most high-resolution imaging or in situ experimentation. To truly be useful in common experiments, a more powerful "closed-loop" approach is required. In this approach, the microscope system performs on-the-fly human-like reasoning to detect changes relative to control set points, such as the movement to a region of interest or changes in a spectrum. This first step requires

Received: December 16, 2022. **Revised:** August 15, 2023. **Accepted:** September 21, 2023
© The Author(s) 2023. Published by Oxford University Press on behalf of the Microscopy Society of America.
This is an Open Access article distributed under the terms of the Creative Commons Attribution License (https://creativecommons.org/licenses/by/4.0/), which permits unrestricted reuse, distribution, and reproduction in any medium, provided the original work is properly cited.

domain-specific analytics, which has been the topic of many recent studies (Muto & Shiga, 2020; Akers et al., 2021; Ghosh et al., 2022; Treder et al., 2022; Stuckner et al., 2022; Ziatdinov et al., 2022a). However, once an instrument control decision is made it must be implemented precisely. Here, lack of access to user-directed control of the microscope poses major barriers, though sophisticated workarounds have been developed by the community (Carragher et al., 2000; Mastronarde, 2003; Yin et al., 2020). New microscope controllers are beginning to emerge that take advantage of low-level application programming interfaces (APIs), open-source software, and fast computing hardware to direct decision-making (Olszta et al., 2022; Roccapriore et al., 2022).

With the advent of such new controllers, the community must now address the challenge of implementing a control platform that can account for both large volumes of decisions and potential imprecision in their execution. We have recently developed a centralized, asynchronous scanning transmission electron microscope (STEM) control platform that has allowed us to evaluate challenges to self-driving "closed-loop" microscopy (Olszta et al., 2022). As already mentioned, there are many sources of imprecision in microscope control; for example, lens voltages can drift, leading to parasitic aberrations, or mechanical lash can cause hysteresis in stage movements. In practice, this means that thousands of decisions can be made in the span of a few seconds and any error compounds rapidly. It is important to note that in any self-driving experiment, errors in position will grow linearly with the number of movement commands. This is then compounded fivefold due to the number of degrees of freedom that are present with the transmission electron microscope (TEM) (x, y, z, α, and β). Even a 1% error in displacement will translate to being off by a full movement command after 100 steps, unless the motion is actively compensated. Traditionally, human operators would perform learned corrections to these errors as reflexive memory commensurate with years of experience. However, in truly automated microscopy this imprecision must be accounted for algorithmically.

To aid in the development of "closed-loop" control, we must first consider the microscope stage, which is essential for reliable imaging and observation of objects along desired orientations. There are several key characteristics of any stage: freedom of movement, stability, and movement reproducibility. Freedom of movement is largely defined by the geometry of the microscope pole piece and the capabilities of the stage itself (i.e., tilt axes, in situ stimuli, and X-ray background). The static and dynamic stability of the stage are critical factors in both extreme atomic-resolution imaging, as well as during in situ experimentation, where an object must often be tracked or kept within a field of view (Zheng et al., 2015). There are many factors that contribute to stability, including the holder geometry (side entry versus internal stage), sample response, and column temperature, and vendors have spent a great deal of time optimizing stage stability. Unfortunately, the last characteristic, movement reproducibility, has largely been overlooked in the past decades, despite the fact that it is one of the most critical parts of emerging self-driving experimentation. The ability to precisely move to and recall positions is critical for quantitative mapping, adaptive sampling, predictive tilting, and many other desirable experiments. Present automation software must perform tedious and time-consuming iterative correction to compensate for imprecision at even low magnification, or a human must be present to manually reposition the stage when an object leaves the field of view. Such correction is increasingly impractical if we are to move toward more automated and eventually autonomous microscopy.

The development of automated TEM stage movement is thus predicated on a wider acknowledgement of the current limitations of standard holder/goniometer design. Whereas there are numerous research papers aimed at stage calibration in the scanning electron microscopy (SEM), there is little to no such information for TEM. We aim to contribute to the dialogue around the level of stage stability needed for the future of automation.

Here, we provide a mathematical framework to evaluate the precision and accuracy of stage movement in any TEM. Our aim is to provide a systematic approach to evaluate stage performance and identify barriers to fully automated experimentation. We consider the unique characteristics of TEM stages and define appropriate coordinate frames of reference. We then perform systematic automated tests in the TEM specifically, utilizing our AutoEM system to conduct large-scale data collection. We identify sources of error and comment on the considerations for a hypothetical future microscope stage, which will enable unprecedented new scientific discoveries.

Results and Discussion

The ability to accurately predict and control stage motion in the TEM is paramount to achieving automated experiments, such as montaging and tilt series. To understand present challenges, we consider typical hardware designs, shown in Figure 1. Montaging and stage control in EM is often associated with SEM (Fig. 1a), where movement occurs within a Cartesian frame of reference. Considering only translation, these stages generally travel linearly in the x (red arrow) and y (blue arrow) planes, usually along independent rails, with z height (or working distance) achieved by the stage moving linearly in the z direction (green arrow). Due to the larger field of view, linear stage motion, and large chamber designs, considerable research has been conducted in the field of SEMs, with some researchers utilizing ML in montaging protocols to circumvent the inherent difficulties in predicting stage movements (Chalfoun et al., 2017). We note that others have utilized a variety of different methods to perform both image and stage calibrations in the SEM (Fu et al., 1994; Ritter et al., 2006, 2007; Mick et al., 2010; Kuwajima et al., 2013; Zimmermann et al., 2013; Cui & Marchand, 2015; Chalfoun et al., 2017; Pang et al., 2019; Liu et al., 2022). In contrast, the movement of a TEM stage is often confusing because either the end of the holder is encased in a protective covering (in the case of modern microscopes) or only the end of the holder is visible. We have found that users typically assume stage movement in the TEM is linear, as is the case for the SEM, since movement is only observed through cameras or a viewing screen and controls provide linear designations.

TEM stages in fact do not move in a linear fashion, but operate within a spherical coordinate system, as shown in Figure 1b. The x-axis can be considered largely linear, since the sample rod is pushed out by a motor (blue arrow) and the vacuum pulls the holder in to achieve the opposite direction, similar to the linear motion in the SEM. However, the complete motion of the TEM stage occurs within a spherical frame of reference, because the goniometer pushes on the ends of the holder in both the y (red arrow) and z (green arrow) directions. The holder then

Downloaded from https://academic.oup.com/mam/advance-article/doi/10.1093/micmic/ozad108/7313517 by guest on 13 October 2023

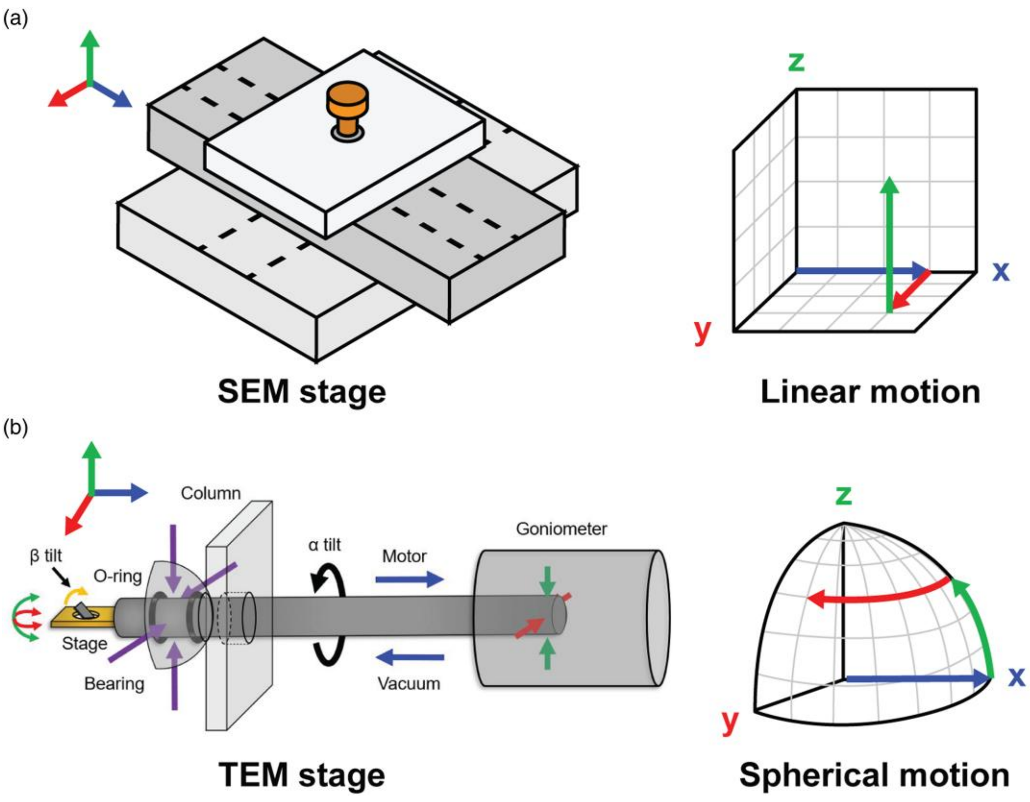

Fig. 1. Overview of electron microscope stages. (**a**) Simplified illustration of the SEM stage and its associated linear frame of reference. (**b**) Simplified illustration of the TEM stage and its associated spherical frame of reference. SEM, scanning electron microscope; TEM, transmission electron microscope.

pivots on an internal hemispherical bearing just inside the column, creating sample motion within a spherical coordinate system. The combination of these three axes makes the prediction of stage movement far more difficult, with microscope manufacturers typically having already calibrated stage motion to appear to travel in a linear manner. We note that, while not shown in the diagram, the motion is further complicated by the addition of α (rotation axis parallel to the long axis) and β (rotation axis perpendicular to the long axis) tilts. When considerations are made for the programming of stage motion, it is important to understand and quantify error associated with such spherical motion. Additionally, while many commercial machines (e.g., lithographic tools and instrumentation found in the semiconductor industry) can operate with nm precision, the current stage design in most modern TEMs also depends on the stifness and consistency of rubber o-rings. This inherent variability provides a challenge to which AI combined with predictive stage movements is necessary. In addition to the variability of the o-rings, there are many other sources of error. These include, but are not limited to, thermal expansion, backlash, hysteresis, gravitational effects, stick-slip, binding, and mechanical oscillations. While a full treatment of every possible source of error is beyond the scope of this text, this work will focus specifically on backlash and hysteresis. This work also focuses on experimental data acquired from TEM stages because of the greater complexity of the design. However, the image processing and alignment techniques described are independent of the type of microscope.

Mathematical Framework

We will now focus on defining a mathematical framework to evaluate stage movement in the TEM specifically; using the terms *target stage position*, *reported stage position*, and *actual stage position* as vernacular. The *target position* is the desired location, or input, as passed from the user to the microscope. The *reported position* is the location reported by the microscope (note this can be further considered as the displayed value or "program" value) after a move command has been completed. The *actual position* is where the sample is located in space as measured by relative displacements between images using cross-correlation image processing techniques, as described in the Materials and Methods section.

To illustrate the possible interactions between these three, several cases are displayed in Figure 2. The first case, shown in Figure 2a, is the ideal case for alignment, where all three terms are commensurate as desired by the user: the target, reported, and actual positions all agree. The remainder of Figure 2 illustrates cases that would be considered misalignment and are representative of most modern goniometer/stage control in TEM. These misalignments are divided into actual, reported, and target, where within various combinations of the three, two of the three positions are aligned with the third being different (Figs. 2b–2d). The next example, shown in Figure 2e, illustrates the case when none of the positions align with each other. While all but the first of these situations are not ideal, if the behavior is repeatable and measurable, then the user can compensate for this misalignment to achieve better performance using predictive algorithms. This compensation is the major differentiator; the final case, Figure 2f, is a situation where it is not possible to compensate for the misalignment. This situation could be due to a time or state dependency, but is most likely a function of the physical state of the holder o-ring due to wear over time.

Downloaded from https://academic.oup.com/mam/advance-article/doi/10.1093/micmic/ozad108/7313517 by guest on 13 October 2023

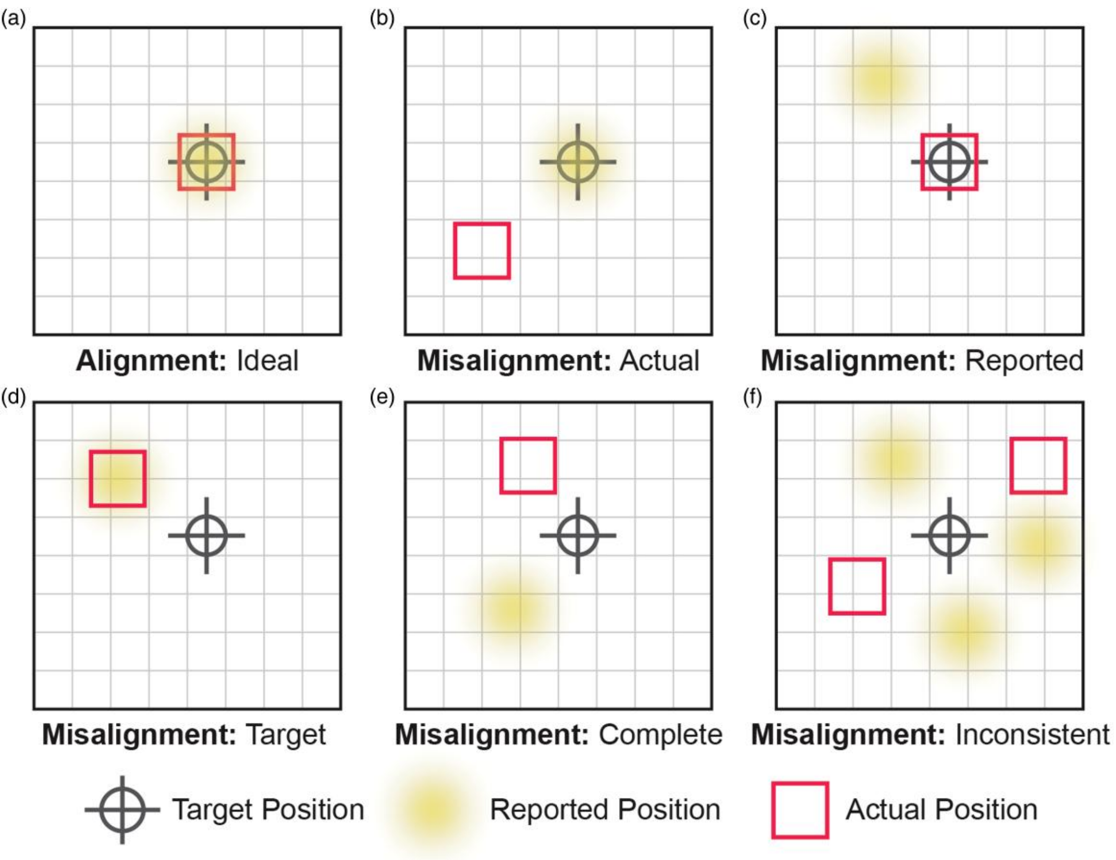

Fig. 2. Framework to analyze possible microscope alignment scenarios. (**a**) Target, reported, and actual positions all coincide. (**b**) Target and reported positions align, actual position is somewhere else. (**c**) Target and actual positions align, reported position is somewhere else. (**d**) Reported and actual positions align, target position is somewhere else. (**e**) None of the target, reported, or actual positions align. (**f**) Target, reported, or actual positions may or may not align in an inconsistent manner. The positions show either large statistical errors or state dependence, such as hysteresis.

Using this nomenclature, the ideal alignment case (Fig. 2a) is the easiest situation where everything works as a user would expect. The next four (Figs. 2b–2f) can be compensated for, and many times are transparent to a user who is manually aligning features of interest. Since a regular user will only interact with the movement relative to the reported value, they can target a region of interest using experience and intuition. However, these situations pose a difficulty if one would like to recall a feature or perform automated, repeatable runs. The final case is the worst, because external analysis cannot compensate or improve microscope behavior. With this vocabulary, the misalignment cases would be considered forms of systematic error on the measurement. This measurement is distinguished from statistical error relating to noise in the reported value or step size. Another way of describing this would be to say that the ideal alignment has accuracy (measured close to the true value), as does Figure 2c. Colloquially, the other cases could be described as inaccurate measurements of the actual position.

Hardware Testing

Having defined these microscope/stage input parameters, as well as the combinatorial possibilities of all three positions, we conducted a set of automated experiments to understand and quantify stage reliability/reproducibility. This approach allows us to assess the feasibility of programming autonomous modules and also enables comparisons against stages across vintage, institution, company, or microscope. We specifically outline an analysis framework where a user can understand which case their microscope exhibits and what can be done to compensate for any misalignment that is present. Generally, the idea is to complete pairwise comparisons between different position measurements (target versus reported, target versus actual, and reported versus actual). These should be evaluated with respect to both the consistency of measurements and whether the stage exhibits state dependence. It is important to note that this can be applied to any EM stage and that the goal of the present study is not to perform a systematic evaluation of trends in microscope stages. A more comprehensive list of experimental considerations can be found in the Supplementary Section 1 and more testing results are in Supplementary Section 2 and Supplementary Section 3.

To check for hysteresis on an axis, the microscope must make repeated moves in a direction and check to see if all the step sizes are the same. For the x and y directions, one can see the results of comparing the target and reported positions, as shown in Figure 3. For each direction, a sequence of five steps was taken. At each location an image was acquired and the reported position of the microscope noted; then a movement command was issued to move to the next position. In this figure, the difference between the reported and target position is plotted against the reported value for that axis. Generally, the agreement is fairly good, but the first step in a

Downloaded from https://academic.oup.com/mam/advance-article/doi/10.1093/micmic/ozad108/7313517 by guest on 13 October 2023

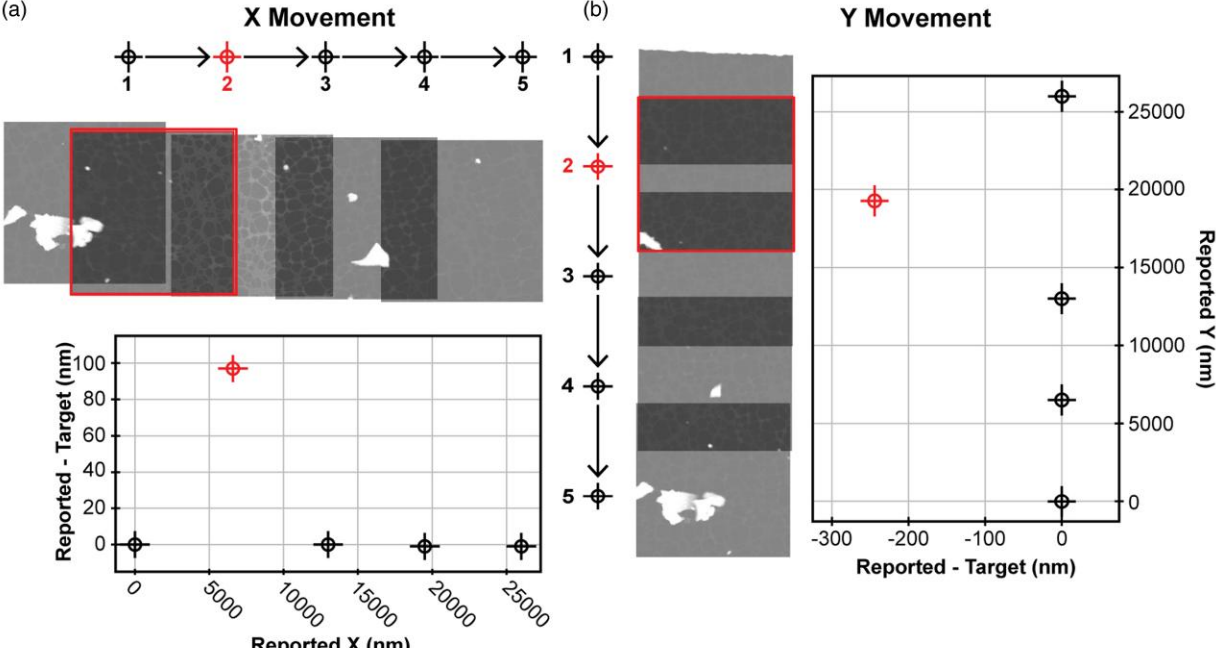

Fig. 3. Hysteresis testing for independent axes. (**a**) Hysteresis test for movement in the *x* direction. (**b**) Hysteresis test for movement in the *y* direction. Images were acquired sequentially along a line, and the reported position minus the target position is shown as a function of the reported position for each direction. Each image was acquired at 50, 000× magnification with a field of view of 3.75 by 3.75μm and has been made 50% transparent to illustrate overlaps.

given direction shows a smaller reported displacement than the target. These steps are highlighted in red, and in the overlapped images, these show significantly more overlap than subsequent steps. To demonstrate the quality of the alignment, images in the figure have been made partially transparent. Any misalignment would appear as a blurry edge. The stitched images show a characteristic hysteretic behavior that is often referred to as backlash. In practice, backlash is accounted for by overcompensating in the reverse direction by the human operator, but which must be explicitly programmed for in automated experimentation. If not accounted for, objects can be incorrectly positioned or missed and these errors will accumulate over the course of an automated experiment.

Next, we check to see if movement along one axis impacts the measurements along a different axis, and vice versa. As shown in Figure 1b, movement within a TEM stage is characterized by arcs, not lines. Consequently, movement in an arc will cause displacements in more than one Cartesian axis, which if not accounted for by the microscope hardware or software, could couple movement commands between axes. For completeness, one should check every possible step direction and each possible combination of two. However, in this study we only consider the x and y directions, because these are the ones most easily interrogated for actual position location measurements using cross-correlation techniques to align overlapping features. In this test, linear steps along a direction are interspersed with perpendicular steps as the microscope moves along each cardinal direction, as shown in Figure 4. In this figure, the reported and actual positions are plotted for movement in each cardinal direction to illustrate the discrepancies in the values.

In general, we observe that steps along different axes do not significantly impact the reported locations on other ones. There is still hysteresis on each axis separately, so moving out and back does not return the microscope to the identical position, as can be seen with the inset microscope images. From the actual microscope images shown in Figure 4, it is apparent that the consistency of the reported position values is not reproduced in the actual images. This finding also highlights the fact that inaccuracies at the individual step level can accumulate over multiple move commands to create an overall larger error, where the final image is not the same as the initial image, even if the target or reported positions are identical. This finding indicates that orthogonal movements are largely uncoupled and we can compensate for lash independently. However, we observe that error compounds rapidly and that an object being tracked can move greatly within the field of view unless iterative correction is applied. To summarize the results of the hardware testing applied to our stage, we found that it shows hysteresis when changing directions and that the x- and y-axes are generally uncorrelated beyond this hysteresis. Due to the hysteresis observed in the first step in a given direction, there is a history dependence that makes general compensation of the motion to improve accuracy challenging. Within the general analysis framework shown in Figure 2, our stage is in the category of "Misalignment: Inconsistent" shown in Figure 2f.

Conclusions

Here, we have provided a general framework to evaluate stage movement within any TEM. We show that there is coupling among axes of movement in the TEM, which operates in a spherical coordinate system that is much more complex than the Cartesian system commonly understood from SEM. We observe several potential complications for automated movement within this spherical frame of reference, owing to coupling of axes and imprecision in mechanical motion.

Downloaded from https://academic.oup.com/mam/advance-article/doi/10.1093/micmic/ozad108/7313517 by guest on 13 October 2023

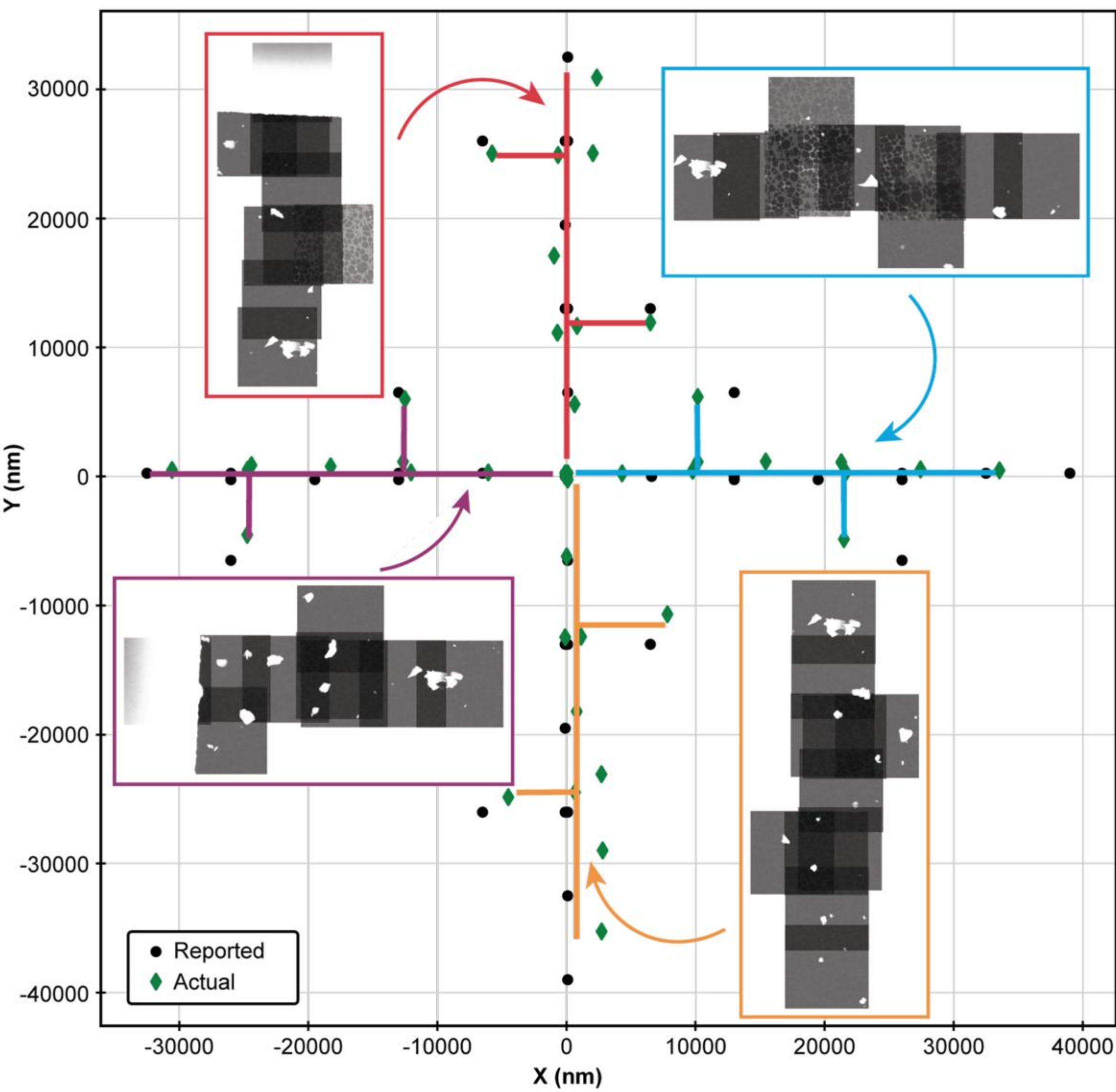

Fig. 4. Hysteresis testing for coupled orthogonal axes. Reported and actual locations for two-axis correlation acquisitions. Each cardinal direction moves from the origin outward and has the images overlapped at 50% transparency to visualize the overlap. Each image was acquired at 50, 000× magnification with a field of view of 3.75 by 3.75μm.

Understanding this relationship is critical for emerging automated microscope systems and is particularly relevant for high-speed experimentation, where rapid movements must be made in sequence to track an object or reaction.

The analysis framework described here provides several concrete pieces of information relating to TEM stage motion. First, we found that in general, the target, reported, and actual position of the microscope might disagree with each other. Next, we identified that the first step in a given direction shows different behavior than repeated steps in that direction and this information can be used effectively in automation experiments. We observed that the *y*-axis tended to be more stable than the *x*-axis for our particular stage, indicating that it is important to map the characteristics of each holder. If there is a particular orientation where accuracy is more important in future experiments, for example, then this axis can be roughly aligned along the *y*-axis for improved performance as compared to a random alignment within the microscope. We emphasize that this analysis framework is general and our findings do not speak to overall relative performance of any specific holder design.

In general, we conclude that active feedback on the stage position in relation to regions of interest is essential to achieve automated human-level performance using present stages. This feedback may be provided through software correction, but it is more desirable to eliminate imprecision at the hardware level. It is likely that full automation will be some combination of physical hardware and AI improvement. Currently, the reported stage position is merely inferred from the signal that is sent to the motors. This situation leaves an information gap within the system between the targeted and actual position, in addition to the misalignment reported for the system. Moving forward, we will wish to design new stages with precise, scalable movements, specifically incorporating independent axis control, accurate positioning feedback, as well as in situ stimuli needed for rich, automated experimentation. Such designs will no doubt be challenging to create, but they are an essential step toward breakthrough discoveries in the age of automation. This research aims to motivate wider conversation in regards to stage stability, with the ultimate goal of development of automated TEM platforms,

Downloaded from https://academic.oup.com/mam/advance-article/doi/10.1093/micmic/ozad108/7313517 by guest on 13 October 2023

whether through re-design of the stage or algorithms to improve upon present imprecision.

Materials and Methods

Hardware

The microscope used in the main text of this study is a customized probe-corrected JEOL GrandARM-300F STEM equipped with the AutoEM platform, that allows access and automation of low level controls such as magnification, tilt, and translation (Olszta et al., 2022). The data shown in the main text was acquired in STEM mode at 300 kV accelerating voltage at 50, 000× magnification. Additional data in Supplementary Section 3 was acquired on a JEOL ARM-200CF microscope. The images were acquired in STEM mode at 200 kV accelerating voltage at 20, 000× magnification. In both cases, data processing is performed on a separate remote Dell Precision T5820 Workstation equipped with a Intel Xeon W-2102 2.9 GHz processor and 1 GB NVIDIA Quadro NVS 310 GPU. A JEOL low X-ray background double tilt holder was utilized in these experiments. The exact sequence of measurements for each calculation is given in Supplementary Section 1. Each microscope magnification was calibrated for the dimensions of the total field of view using a Ted Pella MAG*I*CAL® Calibration Standard.

Automated Data Collection

The automation system is composed of interlinked hardware–software components, as described elsewhere (Olszta et al., 2022). HubEM acts as the main end-use application for the system. It serves as a point for entering configuration, storing data, and directing the cooperation of other components through inter-process communication. It is implemented in C#/Python and uses Python.NET 2.5.0, a library that allows Python scripts to be called from within a .NET application. PyJEM Wrapper is an application that wraps the PyJEM 1.0.2 Python library, allowing communication to the TEMCenter control application from JEOL. It is written in Python and runs on the JEOL PC used to control the instrument. GMS Python allows communication to the Gatan Microscopy Suite (GMS) 3.4.3. It runs as a Python script in the GMS embedded scripting engine. All components communicate using a protocol based on ZeroMQ and implemented in PyZMQ 19.0.2.

Image Registration

Overlapping images were aligned using a custom Python 3.7.1 script that implements a normalized cross-correlation technique, as described in Olszta et al. (2022). In brief, the images were converted to grayscale, normalized to have zero mean pixel intensity and maximum absolute pixel intensity of 1. The cross-correlation was computed using the SciPy 1.7.3 library (Virtanen et al., 2020). Peak values in the cross-correlation were used to determine optimal alignment and the actual positions reported in the text.

Availability of Data and Materials

The image data shown and calculations of error are available on FigShare at: https://doi.org/10.6084/m9.figshare.21735797.v2.

Supplementary Material

To view supplementary material for this article, please visit https://doi.org/10.1093/micmic/ozad108.

Acknowledgments

The authors would like to thank Dr. Bethany E. Matthews for reviewing the manuscript.

Author Contributions Statement

K.R.F., M.J.O., D.H., S.A., and S.R.S. conceived and developed the research plan. K.H.Y. and M.J.O. conducted on-instrument testing. K.R.F., D.H., and C.D. programmed the testing routines. All authors contributed to the writing and editing of the manuscript.

Financial Support

This work was supported by the Energy Storage Materials Initiative Laboratory Directed Research and Development program at Pacific Northwest National Laboratory (PNNL). PNNL is a multiprogram national laboratory operated for the U.S. Department of Energy by Battelle Memorial Institute under Contract No. DE-AC05-76RL0-1830. The AutoEM system is located in the Radiological Microscopy Suite in the Radiochemical Processing Laboratory at PNNL.

Conflict of Interest

The authors declare that they have no competing interest.

References

Akers S, Kautz E, Trevino-Gavito A, Olszta M, Matthews BE, Wang L, Du Y & Spurgeon SR (2021). Rapid and flexible segmentation of electron microscopy data using few-shot machine learning. *Npj Comput Mater* **7**, 187. https://www.nature.com/articles/s41524-021-00652-z.

Batra R, Song L & Ramprasad R (2021). Emerging materials intelligence ecosystems propelled by machine learning. *Nat Rev Mater* **6**, 655–678. https://www.nature.com/articles/s41578-020-00255-y.

Battineni G, Sagaro GG, Chinatalapudi N & Amenta F (2020). Applications of machine learning predictive models in the chronic disease diagnosis. *J Pers Med* **10**, 21. https://www.mdpi.com/2075-4426/10/2/21.

Butler KT, Davies DW, Cartwright H, Isayev O & Walsh A (2018). Machine learning for molecular and materials science. *Nature* **559**, 547–555. http://www.nature.com/articles/s41586-018-0337-2.

Carragher B, Kisseberth N, Kriegman D, Milligan RA, Potter CS, Pulokas J & Reilein A (2000). Leginon: An automated system for acquisition of images from vitreous ice specimens. *J Struct Biol* **132**, 33–45. https://linkinghub.elsevier.com/retrieve/pii/S1047847700943144.

Chalfoun J, Majurski M, Blattner T, Bhadriraju K, Keyrouz W, Bajcsy P & Brady M (2017). MIST: Accurate and scalable microscopy image stitching tool with stage modeling and error minimization. *Sci Rep* **7**, 4988. https://doi.org/10.1038/s41598-017-04567-y

Cui L & Marchand É (2015). Scanning electron microscope calibration using a multi-image non-linear minimization process. *Int J Optomechatronics* **9**, 151–169. https://doi.org/10.1080/15599612.2015.1034903

Dan J, Zhao X, Ning S, Lu J, Loh KP, He Q, Loh ND & Pennycook SJ (2022). Learning motifs and their hierarchies in atomic resolution microscopy. *Sci Adv* **8**, 1005. https://www.science.org.

Downloaded from https://academic.oup.com/mam/advance-article/doi/10.1093/micmic/ozad108/7313517 by guest on 13 October 2023

Ede JM (2021). Deep learning in electron microscopy. *Mach Learn: Sci Technol* **2**, 011004. http://arxiv.org/abs/2009.08328. https://doi.org/10.1088/2632-2153/abd614

Fu J, Croarkin M & Vorburger T (1994). The measurement and uncertainty of a calibration standard for the SEM. *J Res Natl Inst Stand Technol* **99**, 191–200. https://tsapps.nist.gov/publication/get˙pdf.cfm?pub˙id=820682.

Ghosh A, Ziatdinov M, Dyck O, Sumpter BG & Kalinin SV (2022). Bridging microscopy with molecular dynamics and quantum simulations: An atomAI based pipeline. *Npj Comput Mater* **8**, 74.

Groschner CK, Choi C & Scott MC (2021). Machine learning pipeline for segmentation and defect identification from high-resolution transmission electron microscopy data. *Microsc Microanal* **27**, 549–556.

Kalinin SV, Ziatdinov MA, Hinkle J, Jesse S, Ghosh A, Kelley KP, Lupini AR, Sumpter BG & Vasudevan RK (2021). Automated and autonomous experiment in electron and scanning probe microscopy. *ACS Nano* **15**, 12604–12627. http://arxiv.org/abs/2103.12165.

Kalinin SV, Ziatdinov MA, Spurgeon SR, Ophus C, Stach EA, Susi T, Agar J & Randall J (2022). Deep learning for electron and scanning probe microscopy: From materials design to atomic fabrication. *MRS Bull* **47**, 931–939.

Kuwajima M, Mendenhall JM, Lindsey LF & Harris KM (2013). Automated transmission-mode scanning electron microscopy (tSEM) for large volume analysis at nanoscale resolution. *PLoS ONE* **8**, e59573. https://doi.org/10.1371/journal.pone.0059573

Laanait N, Ziatdinov M, He Q & Borisevich A (2016). Identifying local structural states in atomic imaging by computer vision. *Adv Struct Chem Imaging* **2**, 14. https://doi.org/10.1186/s40679-016-0028-8

Lalmuanawma S, Hussain J & Chhakchhuak L (2020). Applications of machine learning and artificial intelligence for Covid-19 (SARS-CoV-2) pandemic: A review. *Chaos Solit Fractals* **139**, 110059. https://linkinghub.elsevier.com/retrieve/pii/S0960077920304562.

Lewis NR, Jin Y, Tang X, Shah V, Doty C, Matthews BE, Akers S & Spurgeon SR (2022). Forecasting of in situ electron energy loss spectroscopy. *Npj Comput Mater* **8**, 252.

Liu Y, Kelley KP, Vasudevan RK, Funakubo H, Ziatdinov MA & Kalinin SV (2022). Experimental discovery of structure-property relationships in ferroelectric materials via active learning. *Nat Mach Intell* **4**, 341–350. https://www.nature.com/articles/s42256-022-00460-0.

Mastronarde DN (2003). SerialEM: A program for automated tilt series acquisition on Tecnai microscopes using prediction of specimen position. *Microsc Microanal* **9**, 1182–1183. https://www.cambridge.org/core/product/identifier/S1431927603445911/type/journal_article.

Mick U, Weigel-Jech M & Fatikow S (2010). Robotic workstation for AFM-based nanomanipulation inside an SEM. In *2010 IEEE/ASME International Conference on Advanced Intelligent Mechatronics*, pp. 854–859. New York City: Institute of Electrical and Electronics Engineers (IEEE).

Muto S & Shiga M (2020). Application of machine learning techniques to electron microscopic/spectroscopic image data analysis. *Microscopy* **69**, 110–122.

Olszta M, Hopkins D, Fiedler KR, Oostrom M, Akers S & Spurgeon SR (2022). An automated scanning transmission electron microscope guided by sparse data analytics. *Microsc Microanal* **28**, 1611–1621. http://arxiv.org/abs/2109.14772.

Pang S, Zhang X, Zhang X & Lu Y (2019). A magnification-continuous calibration method for SEM-based nanorobotic manipulation systems. *Rev Sci Instrum* **90**, 053706. https://doi.org/10.1063/1.5086940

Ritter M, Dziomba T, Kranzmann A & Koenders L (2007). A landmark-based 3D calibration strategy for SPM. *Meas Sci Technol* **18**, 404–414. https://doi.org/10.1088/0957-0233/18/2/S12

Ritter M, Hemmleb M, Faber P, Lich B & Hohenberg H (2006). SEM/FIB stage calibration with photogrammetric methods. In *ISPRS Commission V Symposium, 'Image Engineering and Vision Metrology' 2006*, http://hdl.handle.net/11420/14517.

Roccapriore KM, Boebinger MG, Dyck O, Ghosh A, Unocic RR, Kalinin SV & Ziatdinov M (2022). Probing electron beam induced transformations on a single-defect level via automated scanning transmission electron microscopy. *ACS Nano* **16**, 17116–17127.

Schmidt J, Marques MRG, Botti S & Marques MAL (2019). Recent advances and applications of machine learning in solid-state materials science. *Npj Comput Mater* **5**, 83. https://doi.org/10.1038/s41524-019-0221-0

Schorb M, Haberbosch I, Hagen WJ, Schwab Y & Mastronarde DN (2019). Software tools for automated transmission electron microscopy. *Nat Methods* **16**, 471–477. https://doi.org/10.1038/s41592-019-0396-9

Sha W, Guo Y, Yuan Q, Tang S, Zhang X, Lu S, Guo X, Cao YC & Cheng S (2020). Artificial intelligence to power the future of materials science and engineering. *Adv Intell Syst* **2**, 1900143. https://doi.org/10.1002/aisy.201900143

Spurgeon SR, Ophus C, Jones L, Petford-Long A, Kalinin SV, Olszta MJ, Dunin-Borkowski RE, Salmon N, Hattar K, Yang WCD, Sharma R, Du Y, Chiaramonti A, Zheng H, Buck EC, Kovarik L, Penn RL, Li D, Zhang X, Murayama M & Taheri ML (2021). Towards data-driven next-generation transmission electron microscopy. *Nat Mater* **20**, 274–279. https://doi.org/10.1038/s41563-020-00833-z

Stuckner J, Harder B & Smith TM (2022). Microstructure segmentation with deep learning encoders pre-trained on a large microscopy dataset. *Npj Comput Mater* **8**, 200.

Treder KP, Huang C, Kim JS & Kirkland AI (2022). Applications of deep learning in electron microscopy. *Microscopy* **71**, i100–i115.

Vasudevan RK, Choudhary K, Mehta A, Smith R, Kusne G, Tavazza F, Vlcek L, Ziatdinov M, Kalinin SV & Hattrick-Simpers J (2019). Materials science in the artificial intelligence age: High-throughput library generation, machine learning, and a pathway from correlations to the underpinning physics. *MRS Commun* **9**, 821–838.

Virtanen P, Gommers R, Oliphant TE, Haberland M, Reddy T, Cournapeau D, Burovski E, Peterson P, Weckesser W, Bright J, van der Walt SJ, Brett M, Wilson J, Millman KJ, Mayorov N, Nelson ARJ, Jones E, Kern R, Larson E, Carey CJ, Polat İ, Feng Y, Moore EW, VanderPlas J, Laxalde D, Perktold J, Cimrman R, Henriksen I, Quintero EA, Harris CR, Archibald AM, Ribeiro AH, Pedregosa F, van Mulbregt P & SciPy 1.0 Contributors (2020). SciPy 1.0: Fundamental algorithms for scientific computing in python. *Nat Methods* **17**, 261–272.

Wilkinson MD, Dumontier M, Aalbersberg IJ, Appleton G, Axton M, Baak A, Blomberg N, Boiten JW, da Silva Santos LB, Bourne PE, Bouwman J, Brookes AJ, Clark T, Crosas M, Dillo I, Dumon O, Edmunds S, Evelo CT, Finkers R, Gonzalez-Beltran A, Gray AJ, Groth P, Goble C, Grethe JS, Heringa J, 't Hoen PAC, Hooft R, Kuhn T, Kok R, Kok J, Lusher SJ, Martone ME, Mons A, Packer AL, Persson B, Rocca-Serra P, Roos M, van Schaik R, Sansone SA, Schultes E, Sengstag T, Slater T, Strawn G, Swertz MA, Thompson M, van der Lei J, van Mulligen E, Velterop J, Waagmeester A, Wittenburg P, Wolstencroft K, Zhao J & Mons B (2016). The FAIR guiding principles for scientific data management and stewardship. *Sci Data* **3**, 160018.

Xu M, Kumar A & LeBeau J (2021). Automating electron microscopy through machine learning and USETEM. *Microsc Microanal* **27**, 2988–2989.

Xu M, Kumar A & LeBeau JM (2022). Towards augmented microscopy with reinforcement learning-enhanced workflows. *Microsc Microanal* **28**, 1952–1960.

Yin W, Brittain D, Borseth J, Scott ME, Williams D, Perkins J, Own CS, Murfitt M, Torres RM, Kapner D, Mahalingam G, Bleckert A, Castelli D, Reid D, Lee WCA, Graham BJ, Takeno M, Bumbarger DJ, Farrell C, Reid RC & da Costa NM (2020). A petascale automated imaging pipeline for mapping neuronal circuits with high-throughput transmission electron microscopy. *Nat Commun* **11**, 4949.

Zheng H, Meng YS & Zhu Y (2015). Frontiers of in situ electron microscopy. *MRS Bull* **40**, 12–18.

Downloaded from https://academic.oup.com/mam/advance-article/doi/10.1093/micmic/ozad108/7313517 by guest on 13 October 2023

Ziatdinov M, Dyck O, Maksov A, Li X, Sang X, Xiao K, Unocic RR, Vasudevan R, Jesse S & Kalinin SV (2017). Deep learning of atomically resolved scanning transmission electron microscopy images: Chemical identification and tracking local transformations. *ACS Nano* **11**, 12742–12752. https://doi.org/10.1021/acsnano.7b07504

Ziatdinov M, Ghosh A, Wong CYT & Kalinin SV (2022a). AtomAI framework for deep learning analysis of image and spectroscopy data in electron and scanning probe microscopy. *Nat Mach Intell* **4**, 1101–1112.

Ziatdinov M, Liu Y, Kelley K, Vasudevan R & Kalinin SV (2022b). Bayesian active learning for scanning probe microscopy: From Gaussian processes to hypothesis learning. *ACS Nano* **16**, 13492–13512.

Zimmermann S, Tiemerding T, Li T, Wang W, Wang Y & Fatikow S (2013). Automated mechanical characterization of 2-D materials using SEM based visual servoing. *Int J Optomechatronics* 7(4), 283–295. https://doi.org/10.1080/15599612.2013.879501

Downloaded from https://academic.oup.com/mam/advance-article/doi/10.1093/micmic/ozad108/7313517 by guest on 13 October 2023

TESCAN TENSOR

Integrated, Precession-Assisted, Analytical 4D-STEM

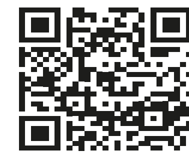

Visit us and learn more
about our TESCAN TENSOR

info.tescan.com/stem